

Alternative Reagents for Methotrexate as Immobilizing Anchor Moieties in the Optimization of MASPIT: Synthesis and Biological Evaluation

Dries J. H. De Clercq,^[a] Martijn D. P. Risseeuw,^[a] Izet Karalic,^[a] Anne-Sophie De Smet,^[b] Dieter Defever,^[b] Jan Tavernier,^[b] Sam Lievens,^{*,[b]} and Serge Van Calenbergh^{*,[a]}

We report the evaluation of two alternative chemical dimerizer approaches aimed at increasing the sensitivity of MASPIT, a three-hybrid system that enables small-molecule target protein profiling in intact human cells. To circumvent the potential limitations related to the binding of methotrexate (MTX) to endogenous human dihydrofolate reductase (DHFR), we explored trimethoprim (TMP) as an alternative prokaryote-specific DHFR ligand. MASPIT evaluation of TMP fusion compounds with tamoxifen, reversine, and simvastatin as model baits, resulted in

dose–response curves shifted towards lower EC₅₀ values than those of their MTX congeners. Furthermore, a scalable azido-TMP reagent was synthesized that displayed a similar improvement in sensitivity, possibly owing to increased membrane permeability relative to the MTX anchor. Applying the SNAP-tag approach to introduce a covalent bond into the system, on the other hand, produced an inferior readout than in the MTX- or TMP-tag based assay.

Introduction

Methods that allow high-throughput identification of the cellular targets of bioactive small molecules are invaluable assets in pharmaceutical research. They are useful in mechanism-of-action studies of hits identified by phenotypic screening, which is increasingly being applied in both academic and industrial programs.^[1] Additionally, they can uncover unexpected targets of established drugs that could contribute to their therapeutic efficacy or cause unwanted side effects (polypharmacology).^[2] Finally, such methods can also lead to the identification of new therapeutic applications of existing drugs within the scope of drug-repositioning projects.^[3] Over the past decade, numerous case studies within the target-profiling field that apply, for example, activity-based protein profiling (ABPP)^[4] or compound-centric chemical proteomics methods (CCCP)^[5] have proved successful. However, despite these success stories, target deconvolution often remains an important bottleneck in drug-discovery research, as a generally applicable methodology is still lacking.^[6]

MASPIT (mammalian small molecule–protein interaction trap) is the three-hybrid component of the MAPPIT technology platform,^[7] which enables the identification of interactions between small organic compounds and their cytosolic target proteins in living human cells (Scheme 1).^[8]

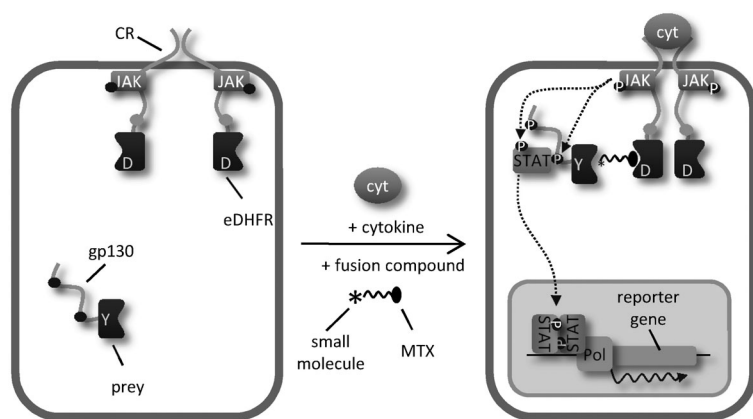
A prerequisite for successful MASPIT analysis is the availability of appropriate synthetic probes. We previously presented a scalable synthesis of a versatile methotrexate (MTX) reagent that allows the rapid γ -selective conjugation to alkyne-functionalized bioactive small molecules to yield MTX fusion compounds (MFCs) appropriate for MASPIT.^[9] Here, we take the next step and discuss our efforts to optimize the MASPIT system's sensitivity based on chemical dimerizers with tamoxifen (TAM) as the model "bait". The latter is a selective estrogen receptor (ER) modulator that has been part of the standard therapy for ER-positive breast cancer treatment since the 1970s.^[10] However, TAM has been reported to induce apoptosis even in ER-negative cancer cells, thus suggesting that it can also operate by modulating alternative targets.^[11] As yet, the exact molecular mechanism of action underlying the apparent promiscuity of this blockbuster drug remains elusive. Taking this together and building on prior experience in constructing and evaluating various TAM-MFCs,^[9] we judged this bait would be a particularly interesting test case for our optimization work.

First, we tried to circumvent any potential limitations related to the tight binding of MTX to endogenous human dihydrofolate reductase (DHFR), which might titrate out a portion of the fusion compound and induce cellular toxicity through perturbation of the endogenous folate metabolism. As an *Escherichia coli* enzyme is employed in MASPIT, we explored trimethoprim (TMP; Scheme 2A) as an alternative prokaryote-specific DHFR ligand. Whereas MTX binds both prokaryotic and mammalian

[a] D. J. H. De Clercq, Dr. M. D. P. Risseeuw, I. Karalic, Prof. Dr. S. Van Calenbergh
Laboratory for Medicinal Chemistry
Faculty of Pharmaceutical Sciences, Ghent University
Ottergemsesteenweg 460, 9000 Gent (Belgium)
E-mail: serge.vanalenbergh@ugent.be

[b] A.-S. De Smet, D. Defever, Prof. Dr. J. Tavernier, Dr. S. Lievens
Cytokine Receptor Laboratory
Department of Medical Protein Research, VIB, Gent and
Department of Biochemistry
Faculty of Medicine and Health Sciences, Ghent University
Albert Baertsoenkaai 3, 9000 Gent (Belgium)
E-mail: sam.lievens@vib-ugent.be

Supporting information for this article is available on the WWW under <http://dx.doi.org/10.1002/cbic.201402702>.



Scheme 1. Outline of the MASPIT system. *E. coli* dihydrofolate reductase (eDHFR) is fused to a cytokine receptor (CR) that is rendered signaling-deficient by mutating STAT3 recruitment sites in its cytoplasmic tail (grey dots). A prey protein is tethered to a gp130 CR fragment containing functional STAT3 transcription factor docking sites (black dots). When a fusion compound consisting of a small molecule of interest (asterisk) coupled to methotrexate (MTX) is added to the cells, MTX binds to eDHFR, resulting in the compound of interest being displayed as bait. Upon administration of the appropriate cytokine ligand (cyt), the CR–eDHFR chimeric receptor undergoes a conformational change, activating the associated JAK2 kinases through cross-phosphorylation (P). Interaction between the small-molecule bait and the prey–gp130 fusion protein brings the latter into proximity of the activated JAK kinases, reconstituting a functional JAK–STAT signaling pathway. Sequential phosphorylation of STAT3 docking sites on the gp130 chain (P), STAT3 recruitment, and STAT3 phosphorylation (P) ultimately leads to activated STAT3 dimers that induce the expression of a luciferase reporter gene coupled to a STAT3-dependent promoter.

DHFR with similar affinity, TMP displays a 12000-fold binding preference for *E. coli* over human DHFR ($K_i = 80 \text{ pM}$ vs. 960 nM), thus reflecting its use as a selective antibiotic in the clinic.^[12] Cornish and Sheetz have previously demonstrated the compatibility of the TMP-tag with mammalian systems for intracellular live-cell imaging.^[13]

Furthermore, so as to stabilize the ternary complex (CR–fusion compound–prey chimera) in order to improve the system's sensitivity, we introduced the concept of covalent bonding into the MASPIT assay, which currently relies on reversible interactions on both ends of the MFCs. As a starting point, we selectively and covalently immobilized the fusion compound to the CR by using a SNAP-tag-based system.^[14] This strategy is centered around the human DNA-repair protein *O*⁶-alkylguanine-DNA alkyltransferase (hAGT). Johnsson and co-workers have exploited the low substrate specificity of this enzyme to covalently label SNAP-tag-fused proteins in vivo with a ligand of interest by conjugating the latter to the *para* position of *O*⁶-benzylguanine (BG).^[14] By fusing hAGT to the cytoplasmic domain of the CR and synthesizing the appropriate BG fusion compound (BGFC), we planned to present a covalently coupled bait small molecule (Scheme 2 B).

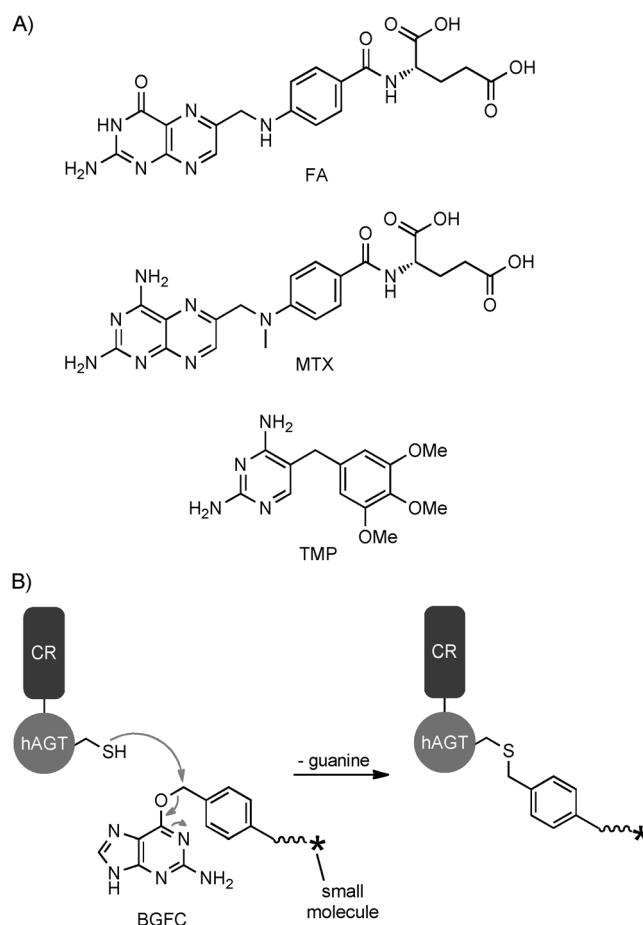
Results and Discussion

TMP-tag approach

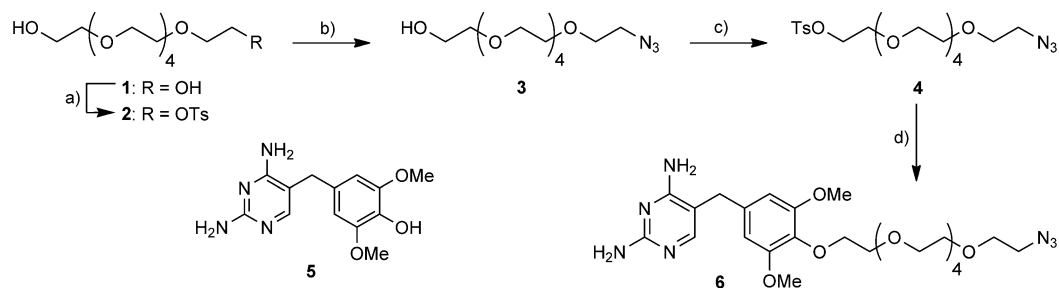
We sought to develop a scalable synthesis of a versatile TMP reagent with an azide ligation handle as an alternative for the earlier MTX congener. A synthetic route towards a first-genera-

tion azido-TMP reagent is depicted in Scheme 3. The synthesis began with the generation of a tosyl/azido bifunctionalized hexa(ethylene glycol) linker (**4**).^[15] This spacer was used to alkylate phenol **5**, which was obtained by acidic hydrolysis of TMP,^[16] to afford the desired ligation handle **6**. However, purification of **6** required RP-HPLC to remove a side product formed by alkylation at the benzhydrylic position (see the Supporting Information). Presumably, this double alkylated TMP analogue was formed by oxidative conversion of phenol **5** to a reactive pyrimidine iminoquinone methide intermediate.^[17] The latter can be converted through resonance stabilization to the corresponding *para*-quinone methide form, which has a prochiral activated exocyclic methylene group. This side reaction rendered this alkylation unsuitable for scale-up. Therefore, we examined alternative alkylation conditions, varying the base (DBU, Na_2CO_3), leaving group (I, OM), solvent (DMF), temperature (RT) and reaction time (16–48 h), but none yielded a more favorable regioselectivity profile.

Subsequently, first-generation trimethoprim fusion compounds (TFCs) **7 a–c** were prepared by ligating



Scheme 2. A) Folic acid (FA) and the DHFR inhibitors methotrexate and trimethoprim; B) Mechanism of hAGT-mediated covalent immobilization of the *O*⁶-benzylguanine fusion compound (BGFC) to the cytokine receptor (CR).



Scheme 3. Synthesis of the first-generation TMP- N_3 reagent **6**. a) TsCl, Et₃N, CH₂Cl₂, 0 °C; b) NaN₃, DMF, 60 °C, 64% over two steps; c) TsCl, Et₃N, CH₂Cl₂, 0 °C, 91%; d) **5**, K₂CO₃, acetone, Δ , 39%.

azido reagent **6** by CuAAC^[18] to the previously described alkyne-functionalized tamoxifen,^[9] reversine^[9] and simvastatin,^[19] respectively (Figure 1). MASPIT evaluation of these TMP conjugates against their established primary target preys showed decreased EC₅₀ values with respect to the corresponding MFCs (Figure 1). These data imply a successful improvement in the system's sensitivity by introducing TMP as an alternative immobilizing anchor moiety, despite the fact that it exhibits lower affinity for eDHFR than MTX ($K_i = 1.0 \mu\text{M}$).^[12]

In a next step, we explored a different alkylation strategy starting from phenol **5** (Scheme 4). Initial alkylations using ethyl 5-bromovalerate in combination with K₂CO₃ consistently provided an intractable mixture of overalkylated products.

Varying the solvent (DMF, acetone), temperature (40 °C, Δ) and reaction time (6–60 h) had negligible effects on the regioselectivity and reaction progress/yield. However, encouraged by the significant positive trend we observed earlier for **6** upon switching to a softer counterion for the carbonate base (K₂CO₃ vs. Na₂CO₃) and further guided by a procedure by Chen et al.,^[20] we ultimately opted for Cs₂CO₃ which successfully gave access to acid **9**. The latter was subsequently condensed with PEG-4 azidoamine **10**^[9] in the presence of 2-(2-pyridon-1-yl)-1,1,3,3-tetramethyluronium tetrafluoroborate (TPTU) to obtain a second-generation azido-TMP reagent in satisfactory yield on a multigram scale. This reagent has the same spacer length, with respect to the number of atoms and chemical

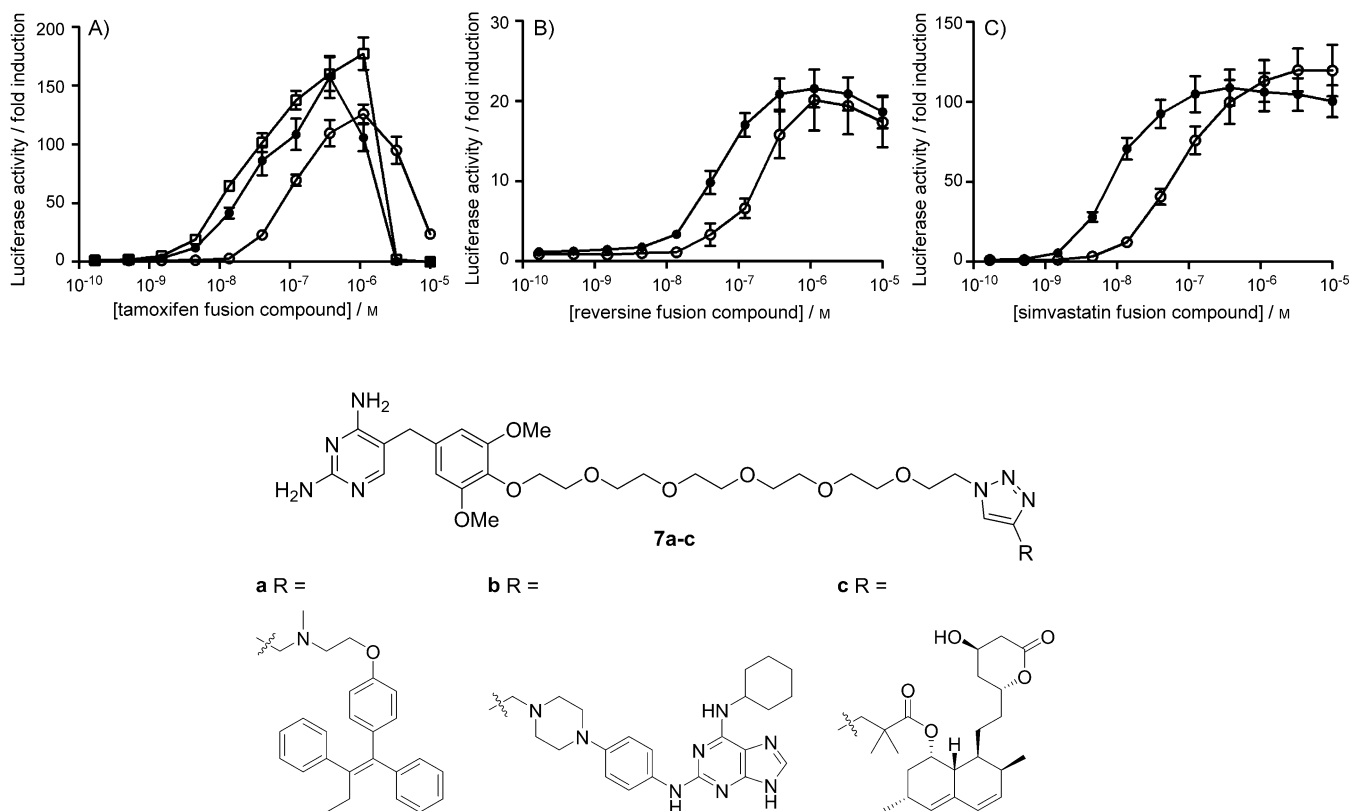
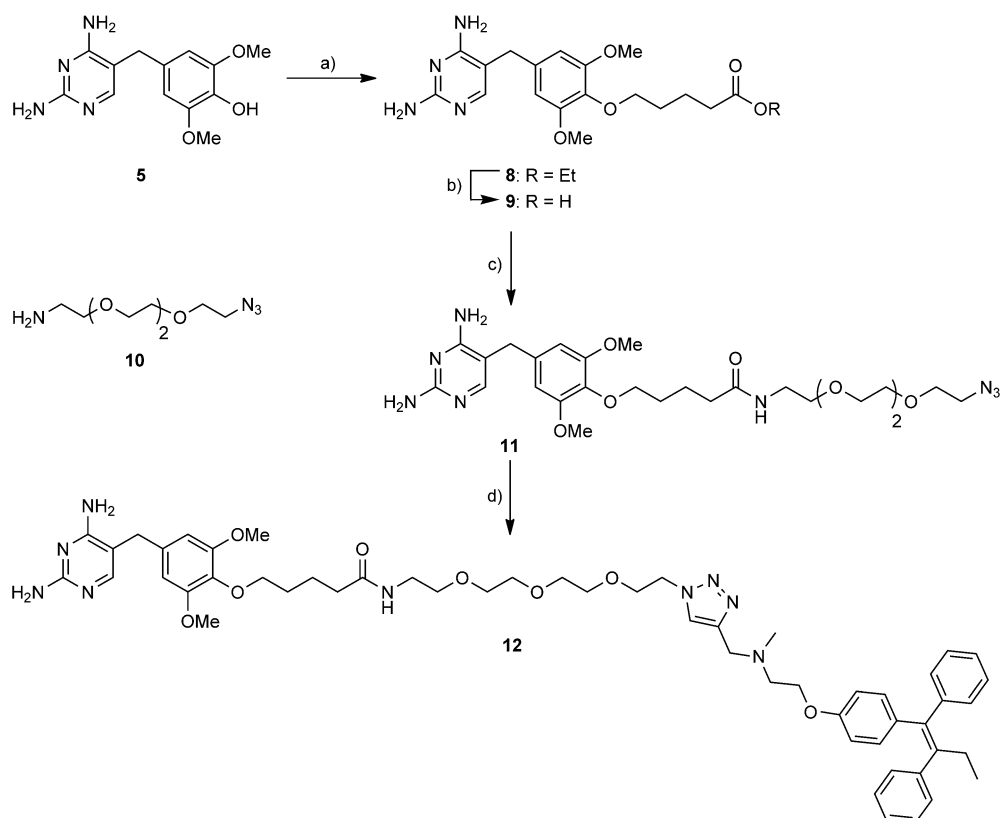


Figure 1. Evaluation of small-molecule TFCs **7a–c** (TMP I, ●) and **12** (TMP II, □) against the corresponding MFCs (MTX, ○) for binding to their primary target protein in MASPIT. A) Tamoxifen–ER1; B) reversine–TTK; C) simvastatin–HMGCR. Luciferase signals are expressed as fold induction relative to a control sample treated with cytokine without fusion compound. In (A), the signal decrease at the highest concentrations is due to the cellular toxicity of the tamoxifen fusion compound (data not shown).



Scheme 4. Synthesis of the second-generation TMP- N_3 reagent **11** and TAM-TFC **12**. a) Ethyl 5-bromovalerate, Cs_2CO_3 , DMF, 70 °C, 66%; b) i: NaOH, MeOH; ii: HCl, 92%; c) **10**, TPTU, Et_3N , DMF, 78%; d) alkyne-functionalized tamoxifen,^[9] CuSO_4 , Na ascorbate, TBTA, $\text{H}_2\text{O}/t\text{BuOH}$, 80 °C, 56%.

bonds, as the original **6** and was analogously click-coupled to the tamoxifen model bait to generate the second-generation TAM-TFC **12**.

Both generations of TAM-TFCs in MASPIT yielded approximately coinciding curves, again shifted towards lower EC_{50} values compared to the original MFC (Figure 1A). Hereby, we demonstrated the biological equivalence of the scalable **11** to **6**, and confirmed the increase in sensitivity for TFCs. Moreover, next to its superior behavior in the MASPIT assay, the newly developed second-generation TMP reagent offers a number of important advantages over the existing MTX anchor from a chemical perspective. The TMP reagent lacks chirality and shows increased solubility, thus making it in general more practical. Furthermore, the reagent has enhanced stability in CuAAC reactions, whereas, under typical conditions, the azido-MTX reagent suffered from significant degradation to the corresponding amine. This is possibly due to residual trifluoroacetic acid in the material from cleavage of the α -*tert*-butylester precursor.^[9] In the case of TMP, which does not require these protecting-group manipulations, CuAACs can be performed without the formation of degradation or by-products, thereby facilitating purification of the final conjugates.

Previously, Cornish^[21] and Bertozzi^[22] obtained contradictory outcomes when comparing the effectiveness of MTX- and TMP-based chemical inducers of dimerization (CIDs) in the same yeast three-hybrid system. For the dexamethasone ligand, Cornish found that the TMP-based CID did not induce

transcription activation as efficiently as the corresponding MTX probe, whereas Bertozzi concluded exactly the opposite for the SLF bait (a synthetic analogue of FK506). They postulated that the disparity in activity between the two CID anchors might be attributed, for example, to different cell-permeability properties. To our knowledge, this aspect has not been experimentally clarified in the context of compound profiling strategies so far. Hence, in an effort to elucidate the origin of the superior performance of TMP fusions in the assay, we studied the uptake of MTX- versus TMP-linked fluorophores in HEK293T cells, the cell line employed in MASPIT. The known azido-MTX and optimized azido-TMP reagents were fused to an alkyne-functionalized BODIPY analogue^[23] by CuAAC to yield **13** and **14**, respectively (Figure 2). Subsequently, the permeability of both conjugates was tracked in a fluorescence-activated cell-sorting (FACS) experiment. First, we measured the fluorescence intensity of both fusion molecules in solution in order to exclude the possibility that the inherent fluorescence of the BODIPY fluorophore was affected by fusion to MTX or TMP. As the concentration–fluorescence curves of both BODIPY fusions closely overlap, this does not seem to be the case (Figure 2A). Next, HEK293T cells were incubated for a fixed time (15 min) with increasing concentrations of either BODIPY fusion molecule. The mean fluorescence of the viable cell subset was measured by FACS, and showed a dose-dependent increase that was significantly higher for the TMP-linked fluorophore than for the MTX fusion molecule (Figure 2B). Addition-

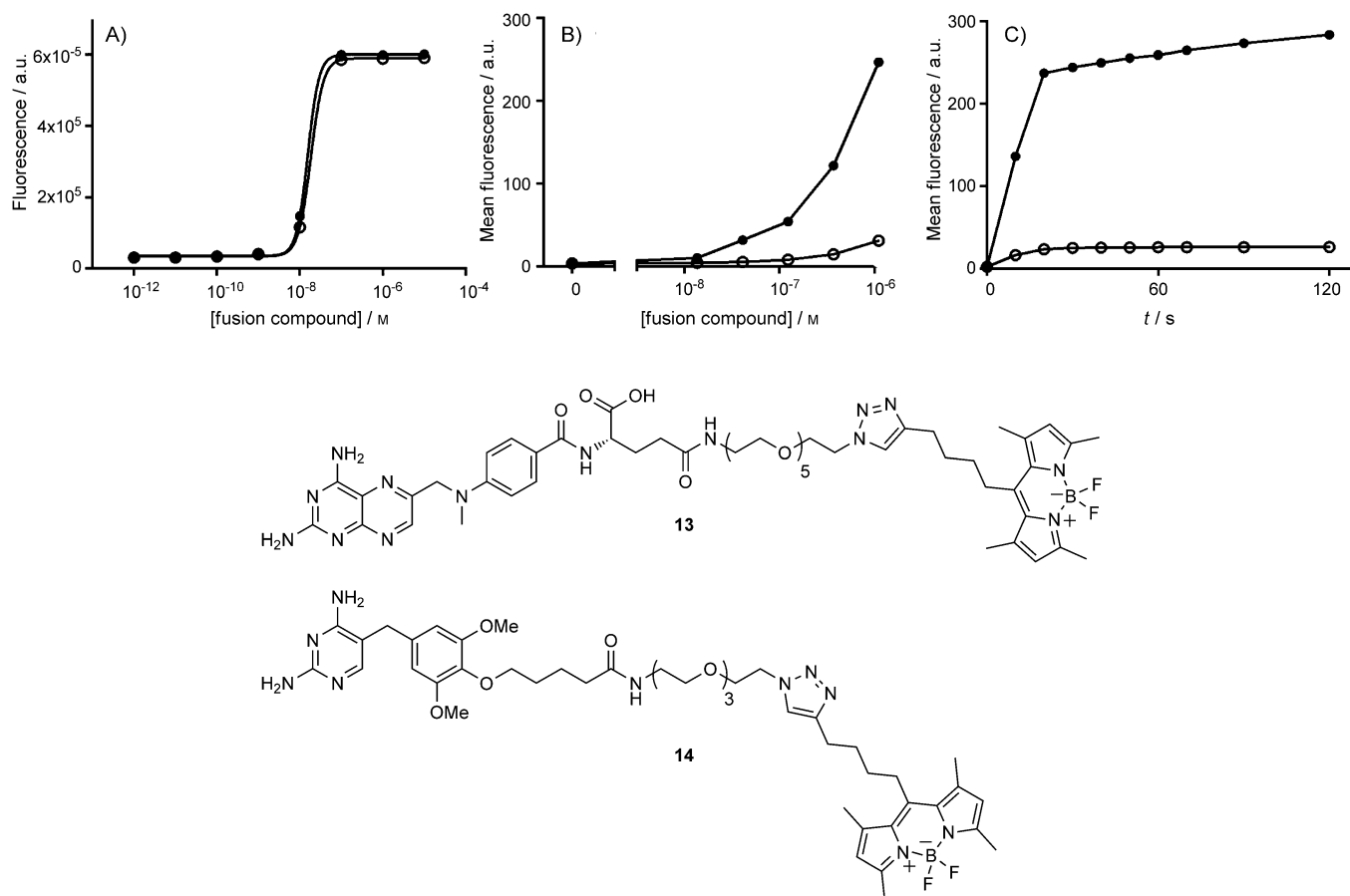


Figure 2. Evaluation of the membrane permeability of BODIPY conjugates of MTX (**13**; ○) and TMP (**14**; ●). A) Dose–response curves showing the inherent fluorescence of the conjugates. B) Dose–response curves of the cellular uptake of the BODIPY conjugates. The graph shows the mean fluorescence as measured by FACS analysis of cells stained with increasing concentrations of the conjugates. C) Kinetic analysis of cellular staining with the MTX- or TMP-BODIPY fusion molecules. Mean fluorescence measured by FACS is plotted against time after the addition of $1 \mu\text{M}$ of either conjugate.

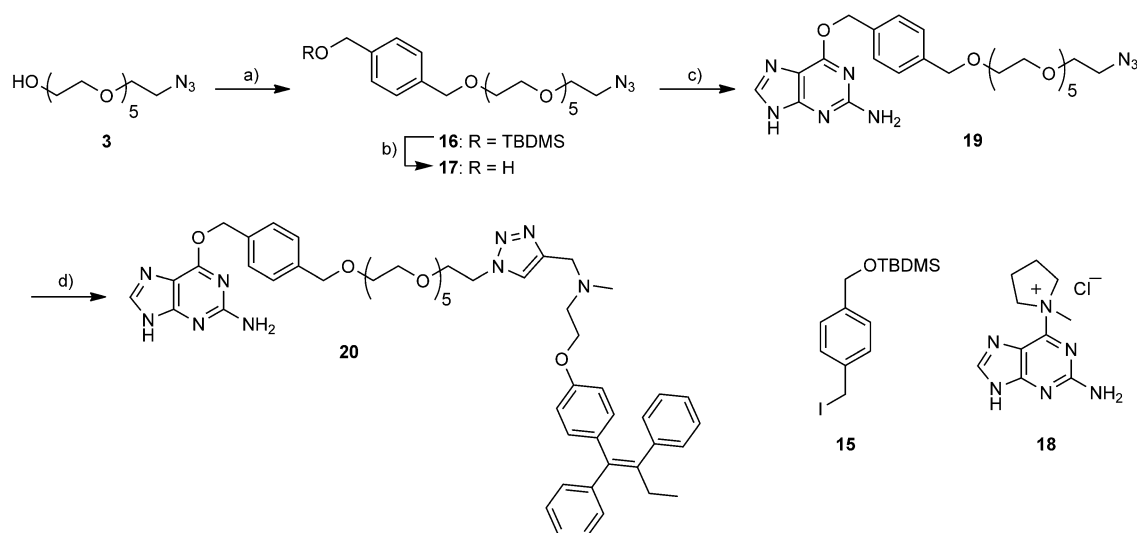
ally, the rate of dye fusion molecule uptake was followed as a function of time at a set concentration of $1 \mu\text{M}$. Cells turned out to take up the BODIPY conjugates rapidly, with maximal fluorescence being reached within 30 s (Figure 2C). Consistent with the dose–response analysis, both the rate of conjugate uptake and the plateau level of fluorescence were markedly higher for the TMP–BODIPY fusion. These results indicate that the increased sensitivity obtained when using TMP fusion compounds in MASPIT can be attributed, at least partly, to a significantly higher membrane permeability than for MTX-linked compounds, although we cannot exclude that this trend might be affected by the nature of the bait.

SNAP-tag approach

To implement the SNAP-tag strategy, we needed a general O^6 -benzylguanine (BG) reagent, *para*-substituted with a PEG linker and with a terminal azide ligation handle. Therefore, the azido spacer **3** was first benzylated and then purinated with **15**^[24] and **18**^[25] respectively (Scheme 5). Subsequent CuAAC between the resulting BG-based building block **19** and alkyne-functionalized tamoxifen readily afforded the desired TAM–BGFC **20**. However, the BG–PEG₆–N₃ reagent suffers from intrinsic

thermal degradation issues that result in the elimination of the terminal azidoethyl group (see the Supporting Information) and make it less attractive than the optimized TMP reagent. In order to enable BGFC incorporation in the MASPIT system, in the plasmid encoding the CR fusion protein, the eDHFR coding sequence was replaced by a DNA fragment encoding a hAGT mutant that exhibits increased activity towards BG and which has been optimized with regard to mammalian codon usage (see the Experimental Section).

The SNAP-tag MASPIT version was evaluated for the interaction between tamoxifen and its primary target, ER1. Cells expressing both the CR–hAGT and ER1 prey fusion proteins and treated with the cytokine ligand and increasing concentrations of the tamoxifen–BGFC **20** exhibited a dose-dependent increase in luciferase reporter activity (Figure 3). This indicated that a ternary complex containing the hAGT and ER1 fusion proteins and the tamoxifen–BGFC is indeed formed, likely involving a covalent bond between hAGT and the BG conjugate. However, the induction window turned out to be significantly lower (sixfold vs. 177-fold) and the EC₅₀ markedly higher ($2.4 \times 10^{-7} \text{ M}$ vs. $2.5 \times 10^{-8} \text{ M}$) than in the case of the TMP-tag setup. Note, we tested a variety of experimental conditions (varying CR–hAGT and ER1 prey expression levels and time between



Scheme 5. Synthesis of BG-PEG₅-N₃ reagent **19** and TAM-BGFC **20**: a) **15**, NaH, DMF, 0 °C, 59%; b) HF-pyr, THF, 80%; c) **18**, KOtBu, DMF, 25%; d) alkyne-functionalized tamoxifen,^[9] CuSO₄, Na ascorbate, TBTA, H₂O/tBuOH, 80 °C, 48%.

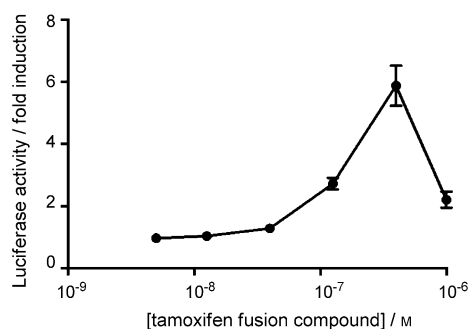


Figure 3. Evaluation of the interaction of TAM-BGFC **20** with ER1 in the SNAP-tag MASPIT setup. The graph shows the fold change in luciferase activity for a concentration gradient of TAM-BGFC relative to a control treated with the cytokine ligand without TAM-BGFC. The signal decrease at the highest concentration is due to the cellular toxicity of the tamoxifen fusion compound (data not shown).

BGFC addition and luciferase readout) for the interaction between the tamoxifen–BGFC and the ER1 prey, as well as several other tamoxifen (off- or on-) target proteins recently identified by our group (S.L., D.J.H.D.C., S.V.C., J.T., unpublished results), and in none of these cases did the SNAP-tag approach perform better than the MTX- or TMP-tag-based assay (data not shown). There might be a number of reasons for this, including titration of the supplied BGFC by endogenous AGT^[14] and CR-hAGT fusion protein degradation upon alkyl transfer.^[26]

Conclusions

In this study, we evaluated two approaches, that is, TMP- and SNAP-tag, to increase the sensitivity of MASPIT. Unexpectedly, the implementation of the SNAP-tag approach, in which the bait fusion molecule is coupled covalently to the CR chimera, did not yield the hypothesized increase in sensitivity. On the other hand, we have demonstrated a clear improvement in the

system's sensitivity by introducing trimethoprim as an alternative immobilizing anchor moiety. This improvement is possibly due to its significantly higher membrane permeability than that of MTX-based fusion compounds. In addition, we presented a scalable synthesis of a versatile TMP reagent that proved superior to the original MTX probe with respect to solubility and stability under various reaction conditions. In a next step, our newly developed second-generation azido-TMP reagent will be applied to uncovering new intracellular targets of small molecules of interest by MASPIT cell-array screening.^[27]

Experimental Section

Synthesis

General: All reactions were performed under nitrogen and at ambient temperature, unless stated otherwise. Reagents and solvents were purchased from Sigma–Aldrich, Acros Organics, or TCI Europe, and used as received. Reactions were monitored by thin-layer chromatography on TLC aluminum sheets (Macherey–Nagel, Alugram Sil G/UV₂₅₄) with detection by spraying with a solution of (NH₄)₆Mo₇O₂₄·4H₂O (25 g L⁻¹) and (NH₄)₄Ce(SO₄)₄·2H₂O (10 g L⁻¹) in H₂SO₄ (10%) or KMnO₄ (20 g L⁻¹) and K₂CO₃ (10 g L⁻¹) in water followed by charring. Column chromatography was performed manually with 60 Å silica gel (Grace, Davisil, 40–63 μm) and/or automatically on a Grace Reveleris X2 flash system equipped with disposable silica gel cartridges (Grace, Reveleris). LC-MS analyses were carried out on a Waters Alliance 2695 XE separation Module by using a Phenomenex Luna reversed-phase C18 column (100×2.00 mm, 3 μm) and a gradient system of HCOOH in H₂O (0.1%, v/v)/HCOOH in CH₃CN (0.1%, v/v) at a flow rate of 0.4 mL min⁻¹. High-resolution spectra were recorded on a Waters LCT Premier XE Mass spectrometer. ¹H and ¹³C NMR spectra were measured on a Varian Mercury-300BB (300/75 MHz) spectrometer. NMR solvents were purchased from Euriso-top. Chemical shifts are given in ppm relative to tetramethylsilane (¹H NMR) or CDCl₃, CD₃OD or SO(CD₃)₂ (¹³C NMR) as internal standards. Preparative TLC purification was carried out on glass-backed Uniplat TLC plates (Analtech, Silica gel GF, UV254, 20×20 cm, 2000 μm). Preparative HPLC purifications were carried

out by using a Laprep preparative RP-HPLC system equipped with a Phenomenex Luna C18 column (21.20×250 mm, 5 μm) with a gradient system of HCOOH in H₂O (0.2%, v/v)/CH₃CN at a flow rate of 17.5 mL min⁻¹.

α-Azido,α-deoxyhexa(ethylene glycol) (3): Triethylamine (8.4 mL, 60.4 mmol) and TsCl (5.62 g, 29.5 mmol) were added to an ice-cooled solution of hexa(ethylene glycol) (9.58 g, 33.9 mmol) in anhydrous CH₂Cl₂ (150 mL). This solution was stirred overnight, and the temperature was allowed to rise to RT. The reaction mixture was concentrated in vacuo, and the crude tosylate was taken up in DMF (250 mL). Sodium azide (6.71 g, 103.2 mmol) was added, and the mixture was vigorously stirred overnight at 60 °C. The mixture was concentrated in vacuo, and the residue was purified by silica gel chromatography (MeOH/CH₂Cl₂ 2:98, v/v) to yield the title compound (5.80 g, 18.9 mmol, 64%) as a pale yellow viscous liquid. ¹H NMR (300 MHz, CDCl₃): δ = 3.74–3.69 (m, 2H), 3.69–3.64 (m, 18H), 3.62–3.58 (m, 2H), 3.39 (t, *J* = 5.0 Hz, 2H), 3.05 ppm (brs, 1H); ¹³C NMR (75 MHz, CDCl₃): δ = 72.5, 70.5–70.3 (wide peak), 70.2, 69.9, 61.5, 50.5 ppm; HRMS: calcd for C₁₂H₂₅N₃O₆Na: 330.1636 [M+Na]⁺, found: 330.1649.

α-Azido,α-deoxy,ω-p-toluenesulfonylhexa(ethylene glycol) (4): Alcohol **3** (1.53 g, 5.0 mmol) was dissolved in anhydrous CH₂Cl₂ (25 mL), and the solution was cooled on ice. Triethylamine (2.1 mL, 15.1 mmol) and TsCl (2.38 g, 12.5 mmol) were added. The resulting mixture was stirred overnight, and the temperature was allowed to rise to RT. The mixture was concentrated in vacuo, and the residue was purified by silica gel chromatography (MeOH/CH₂Cl₂ 1–3%, v/v) to yield the title compound (2.10 g, 4.5 mmol, 91%) as a brownish-yellow viscous liquid. ¹H NMR (300 MHz, CDCl₃): δ = 7.79 (d, *J* = 8.4 Hz, 2H), 7.35 (d, *J* = 8.4 Hz, 2H), 4.15 (t, *J* = 5.0 Hz, 2H), 3.70–3.56 (m, 20H), 3.37 (t, *J* = 5.0 Hz, 2H), 2.44 ppm (s, 3H); ¹³C NMR (75 MHz, CDCl₃): δ = 144.6, 132.8, 129.7, 127.7, 70.5–70.2 (wide peak), 69.8, 69.1, 68.4, 50.4, 21.4 ppm; HRMS: calcd for C₁₉H₃₅N₄O₈S: 479.2170 [M+NH₄]⁺, found: 479.2176.

First-generation TMP-N₃ reagent (6): K₂CO₃ (138 mg, 1.00 mmol) and PEG linker **4** (369 mg, 0.80 mmol) were added to a solution of phenol **5**^[16] (138 mg, 0.50 mmol) in acetone (5 mL). The resulting mixture was refluxed at 75 °C for 60 h with vigorous stirring. After being cooled to RT, the mixture was concentrated in vacuo. The residue was repeatedly purified by silica gel chromatography (MeOH/CH₂Cl₂ 0–15%, v/v) to give a semipure product, which was further purified to homogeneity by preparative RP-HPLC (10–100% MeCN) to yield the title compound (111.2 mg, 197 μmol, 39%) as a clear, colorless oil. ¹H NMR (300 MHz, CD₃OD): δ = 7.35 (s, 1H), 6.54 (s, 2H), 4.05 (t, *J* = 4.8 Hz, 2H), 3.79 (s, 6H), 3.77–3.71 (m, 2H), 3.71–3.60 (m, 20H), 3.35 ppm (t, *J* = 5.0 Hz, 2H); ¹³C NMR (75 MHz, CD₃OD): δ = 164.9, 161.3, 154.8, 151.8, 136.4, 136.0, 108.8, 106.9, 73.4, 71.5–71.4 (wide peak), 71.34, 71.27, 71.0, 56.6, 51.8, 34.3 ppm; LC-HRMS: *t*_R = 5.90 min (10–100% MeCN, 15 min run); HRMS: calcd for C₂₅H₄₀N₇O₈: 566.2933 [M+H]⁺, found: 566.2919.

First-generation tamoxifen TFC (7a): Azide **6** (166.5 mg, 294 μmol, 2.3 equiv) was taken up in H₂O/*t*BuOH (2.5 mL, 1:1, v/v), and alkyne-functionalized tamoxifen^[9] (50.0 mg, 126 μmol, 1.0 equiv), CuSO₄ (50.4 μL, 0.5 M, 0.2 equiv), and Na ascorbate (252 μL, 0.5 M, 1.0 equiv) were added. The resulting mixture was charged with a catalytic amount of tris((1-benzyl-1*H*-1,2,3-triazol-4-yl)methyl)amine (TBTA)^[28] and heated to 80 °C for 16 h with vigorous stirring. After being cooled to RT, the solution was concentrated in vacuo. The residue was purified by preparative RP-HPLC (10–100% MeCN) to yield the title compound (90.9 mg, 95 μmol, 75%) as a white amorphous solid. LC-HRMS: *t*_R = 6.96 min (10–100%

MeCN, 15 min run); HRMS: calcd for C₅₃H₇₀N₈O₉: 481.2627 [M+2H]²⁺, found: 481.2622.

First-generation reversine TFC (7b): Azide **6** (67.9 mg, 120 μmol, 1.7 equiv) was taken up in H₂O/*t*BuOH (2.1 mL, 1:1, v/v), and alkyne-functionalized reversine^[9] (30.3 mg, 70 μmol, 1.0 equiv), CuSO₄ (28.0 μL, 0.5 M, 0.2 equiv), and Na ascorbate (140 μL, 0.5 M, 1.0 equiv) were added. The resulting mixture was charged with a catalytic amount of both Et₃N and TBTA^[28] and heated to 80 °C with vigorous stirring. Upon completion of the reaction (88 h), the solution was cooled to RT and concentrated in vacuo. The residue was purified by preparative RP-HPLC (10–100% MeCN) to yield the title compound (36.6 mg, 37 μmol, 53%) as a white amorphous solid. LC-HRMS: *t*_R = 5.30 min (10–100% MeCN, 15 min run); HRMS: calcd for C₄₉H₇₂N₁₅O₈: 332.8557 [M+3H]³⁺, found: 332.8524.

First-generation simvastatin TFC (7c): Azide **6** (84.8 mg, 150 μmol, 1.5 equiv) was taken up in H₂O/DMF (3.3 mL, 1:1, v/v), and alkyne-functionalized simvastatin^[19] (42.9 mg, 100 μmol, 1.0 equiv), CuSO₄ (40.0 μL, 0.5 M, 0.2 equiv), and Na ascorbate (200 μL, 0.5 M, 1.0 equiv) were added. The resulting mixture was charged with a catalytic amount of TBTA^[28] and heated to 75 °C for 16 h with vigorous stirring. After being cooled to RT, the solution was concentrated in vacuo. The residue was purified by preparative RP-HPLC (30–50% MeCN) to yield the title compound (16.7 mg, 17 μmol, 17%) as a white amorphous solid. LC-HRMS: *t*_R = 7.39 min (82.03% area under the curve (AUC); see the Supporting Information), 10–100% MeCN, 15 min run); HRMS: calcd for C₅₁H₇₇N₇O₁₃: 497.7784 [M+2H]²⁺, found: 497.7700.

Ethyl 5-(*p*-trimethoprimoxy)valerate (8): Cs₂CO₃ (11.80 g, 36.2 mmol, 2.0 equiv) and ethyl 5-bromovalerate (2.87 mL, 18.1 mmol, 1.0 equiv) were added to a solution of phenol **5**^[16] (5.00 g, 18.1 mmol, 1.0 equiv) in DMF (250 mL). The resulting solution was heated to 70 °C for 7 h. After being cooled to RT, the mixture was concentrated in vacuo, and the residue was purified by silica gel chromatography (MeOH/CH₂Cl₂ 0–13%, v/v) to yield the title compound (4.81 g, 11.9 mmol, 66%) as an off-white solid. ¹H NMR (300 MHz, CD₃OD): δ = 7.51 (s, 1H), 6.50 (s, 2H), 4.11 (q, *J* = 7.1 Hz, 2H), 3.89 (t, *J* = 6.0 Hz, 2H), 3.76 (s, 6H), 3.62 (s, 2H), 2.38 (t, *J* = 7.2 Hz, 2H), 1.87–1.75 (m, 2H), 1.75–1.64 (m, 2H), 1.23 ppm (t, *J* = 7.1 Hz, 3H); ¹³C NMR (75 MHz, CD₃OD): δ = 175.5, 164.4, 163.1, 155.8, 154.8, 136.7, 136.2, 108.1, 106.7, 73.6, 61.4, 56.5, 34.7, 34.5, 30.4, 22.7, 14.6 ppm; HRMS: calcd for C₂₀H₂₉N₄O₅: 405.2133 [M+H]⁺, found: 405.2113.

5-(*p*-Trimethoprimoxy)valeric acid (9): A solution of ester **8** (370 mg, 0.92 mmol, 1.0 equiv) in MeOH (9 mL) was treated with NaOH (1.0 mL, 4.0 M). The resulting mixture was stirred overnight at RT, then neutralized by the addition of HCl (1.33 mL, 3.0 M); this gave fine precipitates. The latter were filtered, washed with a minimal amount of cold MeOH and dried overnight under high vacuum to afford the title compound (317 mg, 0.84 mmol, 92%) as an off-white solid. ¹H NMR (300 MHz, SO(CD₃)₂): δ = 7.51 (s, 1H), 6.54 (s, 2H), 6.09 (s, 2H), 5.71 (s, 2H), 3.77 (t, *J* = 6.0 Hz, 2H), 3.71 (s, 6H), 3.52 (s, 2H), 2.26 (t, *J* = 6.9 Hz, 2H), 1.71–1.54 ppm (m, 4H); ¹³C NMR (75 MHz, SO(CD₃)₂): δ = 174.8, 162.23, 162.18, 155.6, 152.9, 135.7, 134.8, 105.85, 105.76, 71.9, 55.8, 33.8, 33.0, 29.1, 21.3 ppm; HRMS: calcd for C₁₈H₂₃N₄O₅: 375.1674 [M–H]⁻, found: 375.1669.

Second-generation TMP-N₃ reagent (11): TPTU (2.72 g, 9.2 mmol, 1.2 equiv) and Et₃N (10.6 mL, 76.3 mmol) were added to a solution of acid **9** (2.87 g, 7.6 mmol, 1.0 equiv) in DMF (33.5 mL). The resulting preactivation mixture was stirred for 5 min at RT. Subsequently, a solution of spacer **10**^[9] (1.58 g, 7.2 mmol, 0.95 equiv) and Et₃N (10.6 mL, 76.3 mmol) in DMF (4.5 mL) was added dropwise to this

mixture. The resulting reaction mixture was stirred for 5 h at RT, then concentrated in vacuo, and the residue was purified by silica gel chromatography (MeOH/CH₂Cl₂ 0–12%, v/v) to yield the title compound (3.27 g, 5.7 mmol, 78%) as a beige oil. ¹H NMR (300 MHz, CD₃OD): δ = 7.29 (s, 1H), 6.55 (s, 2H), 3.92 (t, *J* = 6.2 Hz, 2H), 3.80 (s, 6H), 3.68–3.57 (m, 12H), 3.54 (t, *J* = 5.6 Hz, 2H), 3.40–3.32 (m, 4H), 2.28 (t, *J* = 7.2 Hz, 2H), 1.87–1.65 ppm (m, 4H); ¹³C NMR (75 MHz, CD₃OD): δ = 176.1, 164.9, 160.8, 154.9, 150.9, 136.8, 135.4, 109.0, 106.9, 73.8, 71.50, 71.49, 71.4, 71.2, 71.0, 70.5, 56.6, 51.7, 40.3, 36.6, 34.2, 30.5, 23.6 ppm; HRMS: calcd for C₂₆H₄₁N₈O₇: 577.3093 [*M*+H]⁺, found: 577.3090.

Second-generation tamoxifen TFC (12): Azide **11** (132.6 mg, 230 μmol, 2.3 equiv) was taken up in H₂O/*t*BuOH (1.6 mL, 1:1, v/v), and alkyne-functionalized tamoxifen^[9] (39.6 mg, 100 μmol, 1.0 equiv), CuSO₄ (40 μL, 0.5 M, 0.2 equiv), and Na ascorbate (200 μL, 0.5 M, 1.0 equiv) were added. The resulting mixture was charged with a catalytic amount of TBTA^[28] and heated to 80 °C for 16 h with vigorous stirring. After being cooled to RT, the solution was concentrated in vacuo. The residue was purified by preparative RP-HPLC (10–100% MeCN) to yield the title compound (54.6 mg, 56 μmol, 56%) as a white amorphous solid. LC-HRMS: *t*_R = 6.98 min (10–100% MeCN, 15 min run); HRMS: calcd for C₅₄H₇₁N₉O₈: 486.7707 [*M*+2H]²⁺, found: 486.7708.

BODIPY MFC (13): The previously described α-*tert*-butylester-protected MTX-PEG₆-N₃ reagent^[9] (79.9 mg, 100 μmol) was taken up in TFA/CH₂Cl₂ (2.2 mL, 1:1, v/v), and the solution was stirred for 40 min at RT. The mixture was then evaporated, coevaporated twice with toluene, and concentrated under high vacuum for 1 h. The resulting deprotected MTX-PEG₆-N₃ reagent residue was taken up in H₂O/DMF (2.6 mL, 1:1, v/v), and CuSO₄ (120 μL, 0.5 M, 0.6 equiv), Na ascorbate (600 μL, 0.5 M, 3.0 equiv), and a catalytic amount of TBTA^[28] were added. Finally, the pH of the resulting reaction mixture was adjusted to 8 by the addition of Et₃N (168 μL, 12 equiv), and BODIPY-alkyne^[23] (108.3 mg, 330 μmol, 3.3 equiv) was added. The reaction mixture was stirred for 24 h at RT and concentrated in vacuo. The residue was purified by preparative RP-HPLC (10–100% MeCN) to yield the title compound (63.7 mg, 59 μmol, 59%) as an orange amorphous solid. LC-HRMS: *t*_R = 7.08 min (10–100% MeCN, 15 min run); HRMS: calcd for C₅₁H₇₁N₁₄O₉BF₂: 536.2789 [*M*+2H]²⁺, found: 536.2791.

BODIPY TFC (14): Azide **11** (57.7 mg, 100 μmol, 1.0 equiv) was taken up in H₂O/DMF (2.6 mL, 1:1, v/v), and BODIPY-alkyne^[23] (75.5 mg, 230 μmol, 2.3 equiv), CuSO₄ (80 μL, 0.5 M, 0.4 equiv), and Na ascorbate (400 μL, 0.5 M, 2.0 equiv) were added. The resulting mixture was charged with a catalytic amount of TBTA^[28] stirred for 29 h at RT, and concentrated in vacuo. The residue was purified by preparative TLC (MeOH/CH₂Cl₂ 1:4, v/v with 1.0% NH₄OH) to yield the title compound (37.0 mg, 41 μmol, 41%) as an orange amorphous solid. LC-HRMS: *t*_R = 7.22 min (10–100% MeCN, 15 min run); HRMS: calcd for C₄₅H₆₅N₁₀O₇BF₂: 453.2544 [*M*+2H]²⁺, found: 453.2533.

α-Azido,α-deoxy,ω-4-((TBDMS)oxy)methyl)benzylhexa(ethylene glycol) (16): Azido spacer **3** (3.63 g, 11.8 mmol, 1.05 equiv) was dissolved in DMF (100 mL), and the solution was cooled on ice under nitrogen. Sodium hydride (60% dispersion in mineral oil, 450 mg, 11.25 mmol, 1.0 equiv) was added to this solution, and the mixture was stirred for 10 min. A solution of compound **15**^[24] (4.28 g, 11.8 mmol, 1.05 equiv) in DMF (20 mL) was then added, and the resulting mixture was stirred overnight; the temperature was allowed to rise to RT. The mixture was then concentrated in vacuo, resuspended in EtOAc (300 mL), and filtered. The filtrate was con-

centrated in vacuo, and the residue was purified by silica gel chromatography (MeOH/CH₂Cl₂ 0–8% v/v) to yield the title compound (3.58 g, 6.6 mmol, 59%) as a clear, colorless oil. ¹H NMR (300 MHz, CDCl₃): δ = 7.30 (brs, 4H), 4.73 (s, 2H), 4.55 (s, 2H), 3.69–3.59 (m, 22H), 3.38 (t, *J* = 5.0 Hz, 2H), 0.94 (s, 9H), 0.09 ppm (s, 6H); ¹³C NMR (75 MHz, CDCl₃): δ = 140.8, 136.9, 127.7, 126.1, 73.1, 70.7–70.5 (wide peak), 70.0, 69.3, 64.8, 50.7, 26.0, 18.4, –5.2 ppm; HRMS: calcd for C₂₆H₅₁N₄O₇Si: 559.3522 [*M*+NH₄]⁺, found: 559.3511.

α-Azido,α-deoxy,ω-4-(hydroxymethyl)benzylhexa(ethylene glycol) (17): A hydrogen fluoride–pyridine complex (HF-pyr; 0.9 mL, 38.5 M, 34.7 mmol, 16.6 equiv) was added dropwise to a solution of compound **16** (1.13 g, 2.1 mmol, 1.0 equiv) in anhydrous THF (30 mL) in a plastic flask. The resulting mixture was gently stirred at RT for 6 h, then neutralized with NaOH (10 mL, 4.0 M). The basic solution was concentrated in vacuo, resuspended in MeOH (40 mL), and filtered. The filtrate was dried over Na₂SO₄, filtered, concentrated in vacuo, and finally coevaporated twice with toluene to remove any traces of pyridine. The residue was purified by silica gel chromatography (MeOH/CH₂Cl₂ 0–8% v/v) to yield the title compound (716 mg, 1.68 mmol, 80%) as a clear, colorless oil. ¹H NMR (300 MHz, CDCl₃): δ = 7.30 (brs, 4H), 4.60 (s, 2H), 4.52 (s, 2H), 3.67–3.57 (m, 22H), 3.34 (t, *J* = 5.0 Hz, 2H), 3.20 ppm (brs, 1H); ¹³C NMR (75 MHz, CDCl₃): δ = 140.6, 137.1, 127.6, 126.6, 72.7, 70.4–70.2 (wide peak), 69.7, 69.1, 64.3, 50.4 ppm; HRMS: calcd for C₂₀H₃₇N₄O₇: 445.2657 [*M*+NH₄]⁺, found: 445.2673.

BG-PEG₆-N₃ reagent (19): Benzyl alcohol **17** (711 mg, 1.66 mmol, 1.0 equiv) was dissolved in DMF (4.2 mL) under nitrogen. KOtBu (746 mg, 6.65 mmol, 4.0 equiv) was added to this solution, and the mixture was stirred for 30 min at RT, turning dark red. After this time, compound **18**^[25] (423 mg, 1.66 mmol, 1.0 equiv) was added slowly, and the resulting mixture was stirred for 22 h at RT. The mixture was concentrated in vacuo, and the residue was purified by silica gel chromatography (MeOH/CH₂Cl₂ 0–10%, v/v) to yield the title compound (227 mg, 0.41 mmol, 25%) as a pale yellow oil. ¹H NMR (300 MHz, SO(CD₃)₂): δ = 7.82 (brs, 1H), 7.48 (d, *J* = 7.8 Hz, 2H), 7.35 (d, *J* = 7.8 Hz, 2H), 6.27 (brs, 2H), 5.48 (s, 2H), 4.50 (s, 2H), 3.61–3.48 ppm (m, 22H); ¹³C NMR (75 MHz, SO(CD₃)₂): δ = 159.9 (weak), 159.7, 155.2 (weak), 138.4, 137.8 (weak), 135.9, 128.4, 127.5, 113.5 (weak), 71.7, 69.86–69.78 (wide peak), 69.70, 69.2, 69.1, 66.5, 50.0 ppm; LC-HRMS: *t*_R = 6.47 min (91.03% AUC, 10–100% MeCN, 15 min run); HRMS: calcd for C₂₅H₃₇N₈O₇: 561.2780 [*M*+H]⁺, found: 561.2735.

Tamoxifen BGFC (20): Azide **19** (227.3 mg, 405 μmol, 3.2 equiv) was taken up in H₂O/*t*BuOH (2.5 mL, 1:1, v/v), and alkyne-functionalized tamoxifen^[9] (50.0 mg, 126 μmol, 1.0 equiv), CuSO₄ (50.4 μL, 0.5 M, 0.2 equiv), and Na ascorbate (252 μL, 0.5 M, 1.0 equiv) were added. The resulting mixture was charged with a catalytic amount of TBTA^[28] and heated to 80 °C for 16 h with vigorous stirring. After being cooled to RT, the solution was concentrated in vacuo. The residue was purified by preparative RP-HPLC (30–100% MeCN) to yield the title compound (58.1 mg, 61 μmol, 48%) as an off-white amorphous solid. LC-HRMS: *t*_R = 7.89 min (10–100% MeCN, 15 min run); HRMS: calcd for C₅₃H₆₇N₉O₈: 478.7551 [*M*+2H]²⁺, found: 478.7526.

Molecular biology

Plasmid constructs: The CR-eDHFR chimeric protein consisting of the full-size mouse leptin receptor F3 mutant fused to *E. coli* DHFR is encoded by the pCLL-eDHFR plasmid described previously.^[9] The pCLG-hAGT plasmid encodes the CR-hAGT fusion protein, which is made up of the extracellular, transmembrane, and membrane-proximal portions of the mouse leptin receptor tethered to

a mutant hAGT protein. This plasmid was generated by amplifying the hAGT coding sequence of the pSNAPf vector (New England Biolabs) by using forward primer 5'-CCCGA GCTCA ATGGA CAAAG ACTGC GAAAT G-3' and reverse primer 5'-GGGGC GGCCG CTTAA CCCAG CCCAG GCTTG CCCAG-3' to introduce a stop codon downstream of hAGT. The amplicon was cloned into the pCLG vector backbone, which has been described previously,^[27] by using SacI and NotI restriction enzymes. The ER1 prey, consisting of full-size ER1 fused N-terminally to a gp130 receptor fragment containing multiple STAT3 recruitment sites, was generated by Gateway recombinatorial cloning (Invitrogen) into a Gateway-compatible pMG1C vector. To generate this destination vector, first the pMet7-Flag Gateway destination vector was made by amplifying the Gateway cassette from the Gateway-compatible pMG1 vector^[27] by using forward primer 5'-CCCCA ATTGA CAAGT TTGTA CAAAA AAGC-3' and reverse primer 5'-GGGTC TAGAC TACTT ATCGT CGTCA TCCTT GTAAT CTTTA ATAA AACCA CTTTG TACAA GAAAG C-3' (the latter containing the Flag epitope coding sequence), and inserting this amplicon into the pMet7 expression vector^[7a] by ligation of the MfeI-XbaI restriction enzyme product into the EcoRI-XbaI cut pMet7 vector. Next, the gp130 coding sequence of the pMG1 vector^[27] was amplified by using forward primer 5'-CCCTT AATTA ACGGA GGGAG TATCT CGACC GTGGT ACACA GTG-3' and reverse primer 5'-GGGTT AATTA ACCCC TGAGG CATGT AGCCG C-3', which was inserted into the PacI site of the pMet7-Flag Gateway destination vector. Finally, the ER1 open reading frame was transferred into the pMG1C destination vector from the ER1 entry clone of the hORFeome collection.^[30] The pMG1-TTK prey plasmid encoding the C-terminal fusion of full-size TTK to the gp130 fragment^[9] and the pMG1-HMGCR plasmid coding for the C-terminal fusion of the statin-binding cytoplasmic domain to the gp130 fragment^[9] have been described elsewhere, as has the STAT3-dependent firefly luciferase reporter pXP2d2-rPAPI-luciferase.^[7a]

MASPIIT assays: HEK293T cells were cultured in 96-well microtiter plates in Dulbecco's modified Eagle's medium supplemented with 10% fetal calf serum, incubated at 37 °C, under 8% CO₂, and transfected with pCLL-eDHFR or pCLG-hAGT CR fusion protein plasmid (10 ng per 96 wells), pMG1C-ER1, pMG1-TTK, or pMG1-HMGCR prey plasmid (100 ng per 96 wells) and pXP2d2-rPAPI-luciferase (5 ng per 96 wells) by applying a standard calcium phosphate transfection method, as described earlier.^[27] Twenty-four hours after transfection, cells were stimulated with leptin (100 ng mL⁻¹ final concentration) alone or in combination with the indicated concentration of fusion compound. After another 24 h, luciferase activity was measured by using the Luciferase Assay System kit (Promega) on a Envision plate reader (PerkinElmer). Luciferase data are the average of three technical replicates, error bars indicate standard deviation.

Fluorescence measurement: The fluorescence of the MTX- and TMP-BODIPY fluorophores was measured by preparing a serial dilution of the molecules in PBS in 96-well microtiter plates, and analyzing the plates in an Envision plate reader equipped with a FITC filter set. Fluorescence data are the average of three replicates, error bars indicate standard deviation. The curve in Figure 2A was fit by using four-parameter nonlinear regression in GraphPad Prism.

FACS analysis: HEK293T cells at a density of 10⁷ mL⁻¹ were incubated with propidium iodide (3 μM), and the indicated concentration of MTX- or TMP-BODIPY (1 μM final concentration in the kinetic experiment in Figure 2C) for the indicated time (15 min in the dose-response experiment in Figure 2B). Samples were analyzed by using a FACSCalibur instrument (BD Biosciences), measur-

ing mean BODIPY fluorescence of the viable cells (propidium iodide negative).

Acknowledgements

J.T. was supported by a grant from IUAP P6/36, and is a recipient of an ERC Advanced grant (CYRE,340941). S.V.C. and J.T. received support from the Fund for Scientific Research-Flanders (FWO-V). D.D.C. obtained a PhD grant from the Special Research Fund of Ghent University (BOF).

Keywords: dimerization · immobilization · MASPIIT · target identification · trimethoprim conjugates

- [1] D. C. Swinney, J. Anthony, *Nat. Rev. Drug Discovery* **2011**, *10*, 507–519.
- [2] A. L. Hopkins, *Nat. Chem. Biol.* **2008**, *4*, 682–690.
- [3] G. Jin, S. T. C. Wong, *Drug Discovery Today* **2014**, *19*, 637–644.
- [4] B. F. Cravatt, A. T. Wright, J. W. Kozarich, *Annu. Rev. Biochem.* **2008**, *77*, 383–414.
- [5] U. Rix, G. Superti-Furga, *Nat. Chem. Biol.* **2009**, *5*, 616–624.
- [6] S. Ziegler, V. Pries, C. Hedberg, H. Waldmann, *Angew. Chem. Int. Ed.* **2013**, *52*, 2744–2792; *Angew. Chem.* **2013**, *125*, 2808–2859.
- [7] a) S. Eyckerman, A. Verhee, J. Van der Heyden, I. Lemmens, X. Van Ostade, J. Vandekerckhove, J. Tavernier, *Nat. Cell Biol.* **2001**, *3*, 1114–1119; b) S. Lievens, F. Peelman, K. De Bosscher, I. Lemmens, J. Tavernier, *Cytokine Growth Factor Rev.* **2011**, *22*, 321–329.
- [8] M. Caligiuri, L. Molz, Q. Liu, F. Kaplan, J. P. Xu, J. Z. Majeti, R. Ramos-Kelsey, K. Murthi, S. Lievens, J. Tavernier, N. Kley, *Chem. Biol.* **2006**, *13*, 711–722.
- [9] M. D. P. Risseeuw, D. J. H. De Clercq, S. Lievens, U. Hillaert, D. Sinnaeve, F. Van den Broeck, J. C. Martins, J. Tavernier, S. Van Calenbergh, *ChemMedChem* **2013**, *8*, 521–526.
- [10] C. K. Osborne, *N. Engl. J. Med.* **1998**, *339*, 1609–1618.
- [11] E. P. Gelmann, *J. Natl. Cancer Inst.* **1996**, *88*, 224–226.
- [12] J. R. Appleman, N. Prendergast, T. J. Delcamp, J. H. Freisheim, R. L. Blakley, *J. Biol. Chem.* **1988**, *263*, 10304–10313.
- [13] L. W. Miller, Y. Cai, M. P. Sheetz, V. W. Cornish, *Nat. Methods* **2005**, *2*, 255–257.
- [14] A. Keppler, S. Gendreizig, T. Gronemeyer, H. Pick, H. Vogel, K. Johnsson, *Nat. Biotechnol.* **2002**, *21*, 86–89.
- [15] M. J. Hynes, J. A. Maurer, *Angew. Chem. Int. Ed.* **2012**, *51*, 2151–2154; *Angew. Chem.* **2012**, *124*, 2193–2196.
- [16] M. J. C. Long, Y. Pan, H.-C. Lin, L. Hedstrom, B. Xu, *J. Am. Chem. Soc.* **2011**, *133*, 10006–10009.
- [17] W. G. Lai, N. Zahid, J. P. Utrecht, *J. Pharmacol. Exp. Ther.* **1999**, *291*, 292–299.
- [18] V. V. Rostovtsev, L. G. Green, V. V. Fokin, K. B. Sharpless, *Angew. Chem. Int. Ed.* **2002**, *41*, 2596–2599; *Angew. Chem.* **2002**, *114*, 2708–2711.
- [19] S. Lievens, S. Gerlo, I. Lemmens, D. J. H. De Clercq, M. D. P. Risseeuw, N. Vanderroost, A.-S. De Smet, E. Ruysinck, E. Chevet, S. Van Calenbergh, J. Tavernier, *Mol. Cell. Proteomics* **2014**, *13*, 3332–3342.
- [20] Z. Chen, C. Jing, S. S. Gallagher, M. P. Sheetz, V. W. Cornish, *J. Am. Chem. Soc.* **2012**, *134*, 13692–13699.
- [21] S. S. Gallagher, L. W. Miller, V. W. Cornish, *Anal. Biochem.* **2007**, *363*, 160–162.
- [22] J. L. Czaplinski, M. W. Schelle, L. W. Miller, S. T. Laughlin, J. J. Kohler, V. W. Cornish, C. R. Bertozzi, *J. Am. Chem. Soc.* **2008**, *130*, 13186–13187.
- [23] M. Verdoes, U. Hillaert, B. I. Florea, M. Sae-Heng, M. D. P. Risseeuw, D. V. Filippov, G. A. van der Marel, H. S. Overkleeft, *Bioorg. Med. Chem. Lett.* **2007**, *17*, 6169–6171.
- [24] G. Gorins, L. Kuhnert, C. R. Johnson, L. J. Marnett, *J. Med. Chem.* **1996**, *39*, 4871–4878.
- [25] M. Kindermann, N. George, N. Johnsson, K. Johnsson, *J. Am. Chem. Soc.* **2003**, *125*, 7810–7811.
- [26] A. Keppler, H. Pick, C. Arrivoli, H. Vogel, K. Johnsson, *Proc. Natl. Acad. Sci. USA* **2004**, *101*, 9955–9959.

- [27] S. Lievens, N. Vanderroost, J. Van der Heyden, V. Gesellchen, M. Vidal, J. Tavernier, *J. Proteome Res.* **2009**, *8*, 877–886.
- [28] T. R. Chan, R. Hilgraf, K. B. Sharpless, V. V. Fokin, *Org. Lett.* **2004**, *6*, 2853–2855.
- [29] Note that the small shoulder peaks upfield of the right aromatic (7.35 ppm) and benzylic (4.50 ppm) proton signals (i.e., the PEG attachment side) originate from the azidoethyl-eliminated product and account for approximately 9% contamination, as estimated from the corresponding peak integrals.
- [30] P. Lamesch, N. Li, S. Milstein, C. Fan, T. Hao, G. Szabo, Z. Hu, K. Venkatesan, G. Bethel, P. Martin, J. Rogers, S. Lawlor, S. McLaren, A. Dricot, H. Borick, M. E. Cusick, J. Vandenhoute, I. Dunham, D. E. Hill, M. Vidal, *Genomics* **2007**, *89*, 307–315.

Received: December 12, 2014

Published online on February 16, 2015